Geophysical Research Letters

RESEARCH LETTER
10.1029/2020GL088351

Key Points:
- Seismicity in the years prior to and immediately before the mainshock form two halves of a "Mogi Doughnut" surrounding the main slip patch
- Mechanical asperity model predicts stress increase where earthquakes are observed
- Slip region correlates with high interseismic locking and a circular gravity low, suggesting that the asperity is controlled by geologic structure

Supporting Information:
- Supporting Information S1

Correspondence to:
B. Schurr,
schurr@gfz-potsdam.de

Citation:
Schurr, B., Moreno, M., Tréhu, A. M., Bedford, J., Kummerow, J., Li, S., & Oncken, O. (2020). Forming a Mogi doughnut in the years prior to and immediately before the 2014 M8.1 Iquique, northern Chile, earthquake. *Geophysical Research Letters*, *47*, e2020GL088351. https://doi.org/10.1029/2020GL088351

Received 9 APR 2020
Accepted 5 AUG 2020
Accepted article online 10 AUG 2020

Forming a Mogi Doughnut in the Years Prior to and Immediately Before the 2014 *M*8.1 Iquique, Northern Chile, Earthquake

B. Schurr[1], M. Moreno[2], A. M. Tréhu[3], J. Bedford[1], J. Kummerow[4], S. Li[5], and O. Oncken[1]

[1]Deutsches GeoForschungsZentrum-GFZ, Section Lithosphere Dynamics, Potsdam, Germany, [2]Departamento de Geofísica, Universidad de Concepción, Concepción, Chile, [3]College of Earth, Ocean, and Atmospheric Sciences, Oregon State University, Corvallis, OR, USA, [4]Department of Earth Sciences, Freie Universität Berlin, Berlin, Germany, [5]Earthquake Research Institute, The University of Tokyo, Tokyo, Japan

Abstract Asperities are patches where the fault surfaces stick until they break in earthquakes. Locating asperities and understanding their causes in subduction zones is challenging because they are generally located offshore. We use seismicity, interseismic and coseismic slip, and the residual gravity field to map the asperity responsible for the 2014 *M*8.1 Iquique, Chile, earthquake. For several years prior to the mainshock, seismicity occurred exclusively downdip of the asperity. Two weeks before the mainshock, a series of foreshocks first broke the upper plate then the updip rim of the asperity. This seismicity formed a ring around the slip patch (asperity) that later ruptured in the mainshock. The asperity correlated both with high interseismic locking and a circular gravity low, suggesting that it is controlled by geologic structure. Most features of the spatiotemporal seismicity pattern can be explained by a mechanical model in which a single asperity is stressed by relative plate motion.

Plain Language Summary At the northern Chile subduction zone, where the oceanic Nazca plate glides several centimeters per year under the South American continent, the two plates got stuck at an irregularity. This irregularity got stressed for more than 100 years until it broke in 2014 in a magnitude 8.1 earthquake. We mapped small earthquakes in the years preceding the large earthquake. We found that small earthquakes formed a ring around the irregularity. First, a half circle formed along the lower side of the irregularity, probably, because the oceanic Nazca plate is pulled down by its own weight and is thus mainly stressing along the lower side. Then, 2 weeks before the largest earthquake, a series of smaller earthquakes closed the circle around the upper side of the irregularity. Finding such irregularities between tectonic plates is important to assess earthquake risk. We also found that the irregularity can be seen in data derived from Earth's gravity field, hinting that it is due to geologic structure.

1. Introduction

Earthquakes are thought to be frictional instabilities on a fault surface. Asperities are patches on this surface defined as frictionally "strong," which stick until suddenly failing when the yield stress is reached (Lay & Kanamori, 1981). The configuration of these asperities is thought to be a main factor determining the distribution, size, and recurrence interval of large earthquakes (Thatcher, 1990). Asperities are generally recognized either by modeling interseismic surface deformation to infer interplate locking or, in hindsight, as being colocated with regions of large coseismic slip. In subduction zones, large asperities are mostly located offshore (e.g., Schurr et al., 2012), and near-fault measurements are almost always onshore; therefore, their location, shape, size, and amplitude are notoriously underconstrained. Despite the significance of asperities, fundamental aspects about their nature are poorly understood: It is not known whether they are persistent over many seismic cycles (Tilmann et al., 2016; Yamanaka & Kikuchi, 2004), caused, for example, by large-scale fault surface topography or frictional heterogeneities due to lithology or rheology in the fault zone, or whether they are ephemeral features controlled by processes such as pore pressure or stress heterogeneities. Although observational capabilities near faults have improved, there is little high-resolution, long-term data that monitor the evolution of an asperity as it prepares to rupture. Stressing an asperity changes the spatiotemporal distribution of background seismicity (Dmowska & Lovison, 1992;

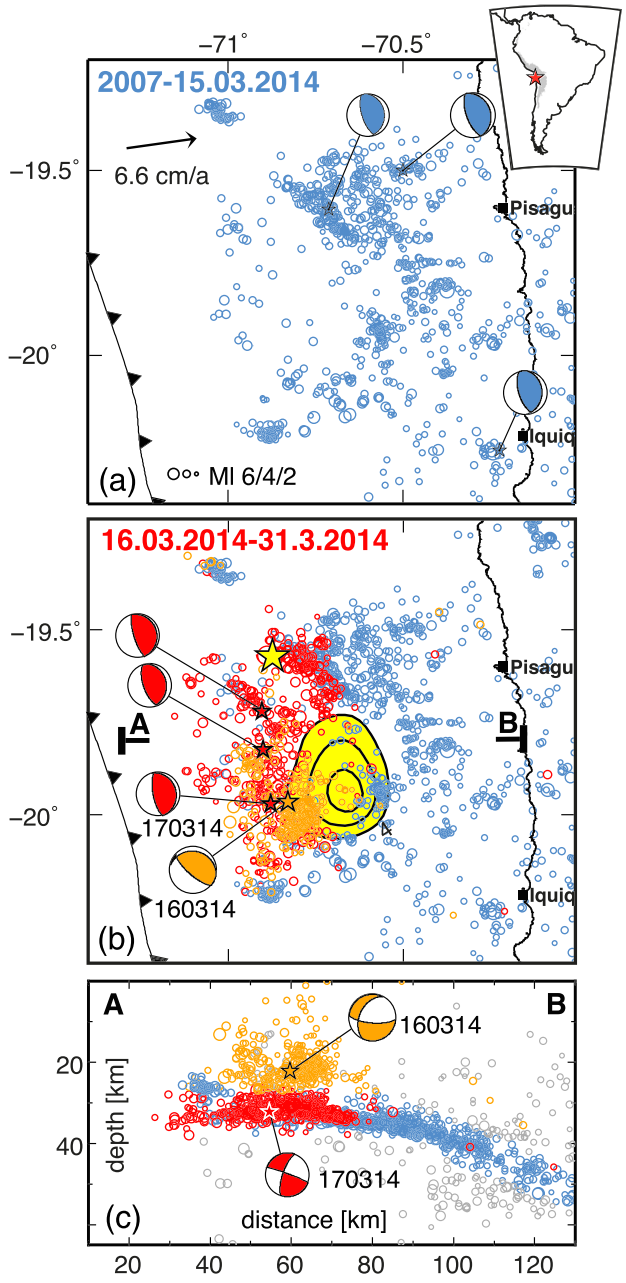

Figure 1. (a) Interseismic seismicity in the Iquique earthquake rupture region on the plate interface (see Figure 1c) from 1 January 2007 to 15 March 2014, that is, 1 day before the *M*6.7 foreshock and 2 weeks before the mainshock. Source mechanisms of earthquakes with *Mw* > 6 are shown as beach balls. (b) Same as (a) but with the preseismic foreshocks added. Presumed upper plate events are orange, and interplate events are red (see Figure 1c). Beach balls for foreshocks with *M* > 6. Location of cross section in Figure 1c) is indicated. Contours mark 6, 9, and 12 m of mainshock slip (Duputel et al., 2015), and yellow star marks mainshock epicenter. (c) Cross section through interseismic and preseismic activity. The two first large foreshocks of *M*6.7 and *M*6.3 are marked with stars and beach balls.

Kanamori, 1981). A detailed analysis of seismicity patterns, therefore, may provide clues about the stress patterns in the fault zone.

The rupture region of the *Mw* 8.1 Iquique earthquake had been monitored for more than 7 years before the mainshock by the Integrated Plate boundary Observatory Chile (IPOC) (GFZ and CNRS-INSU, 2006), providing a unique opportunity to study the spatiotemporal relationships between background seismicity, geodetically derived locking, foreshock activity, and mainshock rupture. Due to the wealth of these observational data, the Iquique earthquake sequence has been extensively studied (e.g., Duputel et al., 2015; Hayes et al., 2014; Herman et al., 2015; Jara et al., 2018; Lay et al., 2014; Meng et al., 2015; Ruiz et al., 2014; Schurr et al., 2014; Soto et al., 2019; Yagi et al., 2014). It broke a central portion of the approximately 500-km-long segment that ruptured last in the great 1877 northern Chile megathrust event (Ruiz & Madariaga, 2018). Published models for the cumulative slip of the mainshock generally agree on a single main slip patch south of the epicenter, which differs in size and amplitude (between, e.g., 4 m, Schurr et al., 2014, and 12 m, Duputel et al., 2015) depending on the choice of inversion method and weighting among the different available data sets (see Duputel et al., 2015, and Figure S1 in the supporting information for examples). The Iquique mainshock was heralded by 2 weeks of intense foreshock activity, which we refer to as the preseismic period, in contrast to the decadal interseismic period (Figures 1 and 2b).

Here we study for the first time the long-term background seismicity in the region of the Iquique earthquake and show that its pattern provides an important missing piece relating the foreshock sequence to a locked asperity and the mainshock rupture. To test our hypothesis that the observed spatiotemporal pattern of seismicity is related to the loading of an asperity, we perform numerical model calculations. We also look at structural features of the forearc as indicators of asperity persistence.

2. Data, Analysis, and Results

2.1. Seismicity

We used the IPOC seismic network and additional permanent and temporary stations in the region to analyze background seismicity in the Iquique source region from 1 January 2007 until the 1 April 2014 mainshock. To detect, locate, and relocate events with sequentially improved phase picks and locations, we used a multistage automatic procedure (Sippl et al., 2013). The catalog differs from the one published by Sippl et al. (2018) in having less stringent event definition criteria at the detection stage and therefore contains more events (3,050 vs. 2,408 events for the map extent of Figure 1b). In the final stage, the catalog was relocated using the double-difference algorithm with cross correlation-based differential travel times (Waldhauser & Ellsworth, 2000).

Seismicity from 1 January 2007 until 15 March 2014 (just before the first large foreshock) is shown in Figure 1a. The region offshore the coastal towns of Pisagua and Iquique was seismically active during the entire observation period, featuring three plate-interface thrust events with $M_w > 6$ in 2008 and 2009, one of which was close to the 2014 mainshock epicenter. Most hypocenters follow a well-defined surface in cross section (Figure S2) downdip of the impending 2014 rupture zone, which we define based on Duputel et al.'s (2015) slip model (Figure 1).

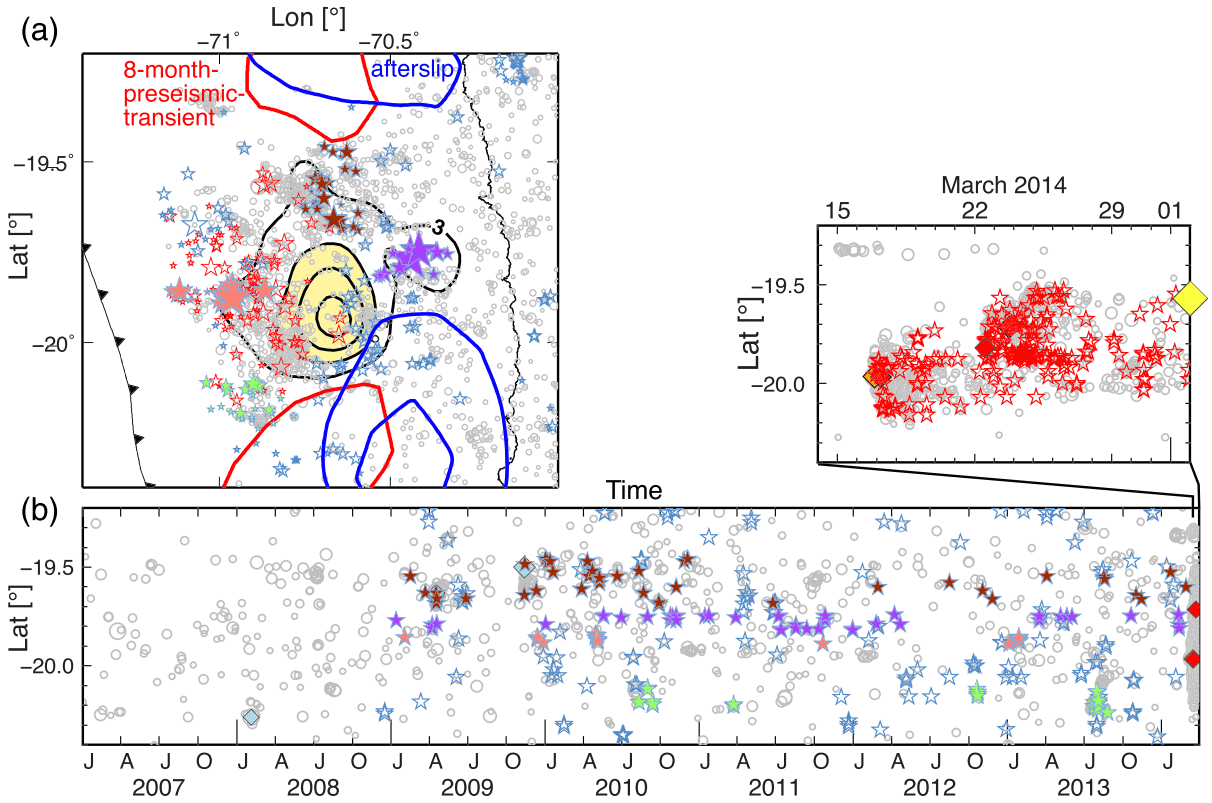

Figure 2. Earthquake repeater analysis. (a) Map view. Stars mark repeater sequences in the interseismic (light blue) and preseismic (red) periods. Symbol size is scaled by number of repeaters per sequence (2–7). Symbol filling allows to identify clusters in (b). Red contours outline 5 mm interseismic (8 months) slip (Socquet et al., 2017), blue contours outline 60/80 cm postseismic slip (Hoffmann et al., 2018). (b) Time versus latitude for preevent seismicity (circles) and repeaters (stars). Colors as in (a). The 2-week foreshock sequence is blown-up above.

On 16 March 2014 a *Mw* 6.7 earthquake initiated the foreshock sequence (Figures 1b and 1c). Within a few hours, another *Mw* 6.3 event broke at ~5-km epicentral distance to the north. Although depth resolution of offshore events is hampered by the lack of offshore stations close to the epicenters, background seismicity preceding the foreshocks defines a landward-dipping plane in cross section, which we interpret as the megathrust (Figures 1c and S2a). The apparent flattening of this plane toward the trench is an artifact of the 1-D velocity model (Husen et al., 1999), placing the offshore events too deeply. The 16 March foreshock clearly locates above this plane, whereas the next largest event (17 March) falls on the plane. The mechanism for the latter event is compatible with interplate motion on the megathrust (Figures 1b and 1c). We corroborate the significant difference in depth and mechanism for these two events by long-period waveform modeling (Nábělek & Xia, 1995), which is less sensitive to the station distribution and velocity model (Figure S3). A similar result has been obtained by Ruiz et al. (2019), where modeled moment tensors with mechanisms similar to the first large foreshock located consistently above mechanisms similar to the mainshock. Over the following days, a cloud of events formed above the plate interface (orange in Figures 1b and 1c), while seismicity on the presumed plate interface (red in Figures 1b and 1c) spread north until it reached the mainshock epicenter (Kato & Nakagawa, 2014; Meng et al., 2015; Yagi et al., 2014) (Figures 1b, 1c, and 2b).

The interseismic events and foreshock sequence form a ring of seismicity that encircles a quiet zone (Figures 1b and S2b). This zone is almost perfectly filled by the high slip (>6 m) patch of the mainshock (Figure 1b). Although we choose here the slip model based on the most complete data set (Duputel et al., 2015), the correlation also holds for other models (Figure S1). Such preseismic patterns, in which a ring of high seismicity surrounds a quiet patch, are known as “Mogi doughnuts” (Kanamori, 1981; Mogi, 1969).

2.2. Repeating Earthquakes

We searched for repeating earthquakes as indicators of fault creep (Igarashi et al., 2003). We used waveforms from the favorably located Station PB11, which started operating in late 2008. As event templates, all events

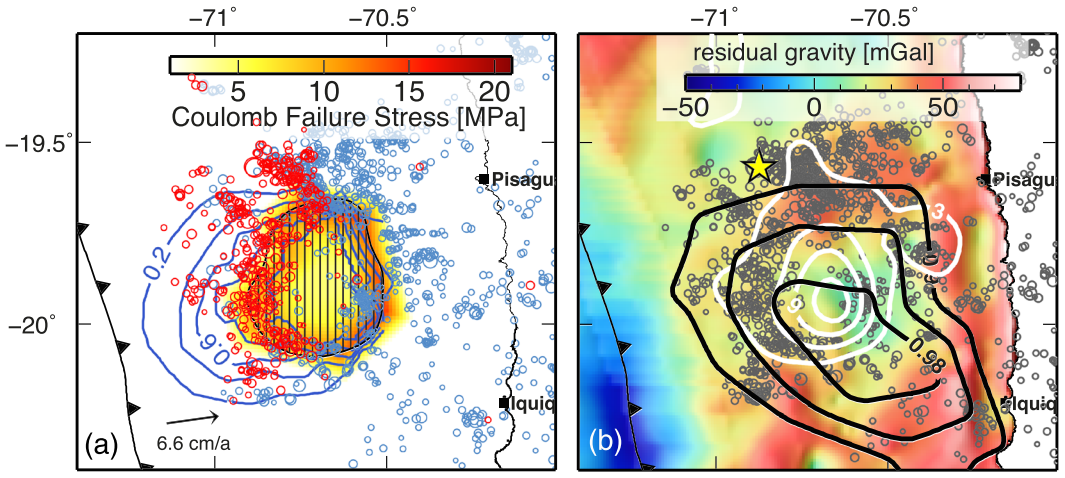

Figure 3. (a) Map with mechanical modeling results. The hashed region is the simulated asperity (3.5 m slip contour, Duputel et al., 2015) that is coupled while the lower plate subducted at plate velocity. Color map is the resulting Coulomb failure stress on the plate interface after 200-year loading. Light blue contours are the resulting locking degree. (b) Residual gravity anomalies, mainshock slip (white contours), interseismic plate locking degree (black), and preevent seismicity (gray).

from the catalog of Sippl et al. (2018), including 9 months of the aftershocks, were used. This inventory covers the subduction fault comprehensively, allowing searching for similar, possibly weak events in regions that were mostly quiet during the interseismic period. For the templates, we cut a 35 s time window starting 5 s before the *P* arrival and including the *S* wave and applied a band-pass filter between 1 and 4 Hz. We classified an event as similar if the normalized cross-correlation coefficient exceeded 0.95.

We identified 432 repeater sequences with up to seven events that were activated before the mainshock (Figure 2). At the northern margin of the asperity, near the epicenter, repeater clusters occurred primarily within a year following two *M*6 events in 2009 and again in summer 2013 and early 2014 (rust colored stars in Figure 2). Updip (west) of the asperity, where few earthquakes occurred during the interseismic period, a number of repeater clusters were active in bursts in early and middle 2010 and early 2013 (orange in Figure 2). The region directly downdip (east) of the asperity contains a streak-like cluster encircled by the 3 m slip contour (purple filled stars in Figure 2). These repeaters were almost continuously active during the observation period (Figure 2b). Assuming that repeaters are loaded by creep, this indicates rather continuous slip at the downdip edge of the asperity. Repeaters in two earthquake streaks south of the asperity (light green) showed highest activity in summer 2013 and later during the foreshock sequence.

2.3. Modeling the Interseismic Locking State

Highs in interseismic locking maps derived by modeling surface displacements provide the most direct indication of megathrust asperities. To obtain a robust locking model and compare it with other attributes of the presumed Iquique asperity, we updated the interseismic locking model of Li et al. (2015) employing the back-slip approach (Savage, 1983; Figure S5a) with viscoelastic Green's Functions, reproducing more realistically forearc deformation (Li et al., 2018). We supplement their model with a combination of new GPS-derived velocities from ~40 continuously recording sites, ~70 survey-type sites and previously published vectors (Figure S4) (Kendrick et al., 2001; Métois et al., 2013). We used a 3-D spherical finite element model (FEM; Figure S5) with a realistic geometry of the subducting slab (Hayes et al., 2012), topography, bathymetry, and the continental Moho boundary (Tassara & Echaurren, 2012). A checkerboard synthetic slip model indicates that anomalies of about 50 km in size can be resolved immediately seaward and landward along the coast but are unresolved and smeared toward the trench (Figure S6). The highest locking degree ($\geq$0.98) correlates with the highest slip zone, which was seismically quiet prior to the mainshock (Figures 3b and S7). This highly locked patch is a robust model feature and can be seen also in other published locking models, albeit differing in size and amplitude (Béjar-Pizarro et al., 2013; Chlieh et al., 2011; Jolivet et al., 2020; Li et al., 2015; Métois et al., 2016; Schurr et al., 2014; Figure S8).

2.4. Interseismic Loading Stresses on the Megathrust and in the Upper Plate

To better understand (a) why the foreshock sequence started in the upper plate and b) the relation between the "Mogi doughnut" seismicity and the presumed asperity, we modeled stresses due to the progressive interseismic loading along the plate interface and its surrounding volume in a 2-D and a 3-D finite element (FE) mechanical model. We simulate the steady interseismic subduction of the oceanic plate implementing a slight modification of the Elastic Subducting Plate Model (Kanda & Simons, 2010; Figure S9), allowing us to model the plate motion and estimating time-varying stresses in the seismogenic zone around a clamped asperity. We simulate the stick-slip behavior by specifying a fault interface with a static friction constitutive model along the seismogenic zone (e.g., Moreno et al., 2018). A higher effective coefficient of friction was used to couple a defined asperity (guided by the coseismic slip model). We applied normal tractions consistent with the overburden (lithostatic load) as initial stress state along the frictional fault. The model produces shear tractions proportional to the fault normal traction plus cohesive stress (Aagaard et al., 2016). For simplicity, our model neglects gravitational body forces and only deals with stress changes as perturbations to the absolute state of background stress.

In a 2-D model the asperity is simulated on the plate interface between depths of 30–40 km (Figure S9a). The resulting surface displacement, plate interface tractions, and plate interface slip following 200 years of simulated time are shown in Figure S10. Modeled horizontal and vertical displacements are consistent with the patterns observed in real subduction zones during the interseismic period (e.g., Kanda & Simons, 2010). The shear tractions on the plate interface are highest at the asperity, especially at the upper and lower edges, with the peak shear traction being at the downdip edge of the asperity. The model predicts increased shear tractions by several MPa in the hanging wall roughly where the first and largest foreshock nucleated (Figure S11).

We apply the general setups of the 2-D model to our 3-D case study using the same model geometry (Figures S9b and S9c) as in the locking inversion. The sense of motion on the simulated megathrust is consistent with the azimuth and rate of plate convergence. We defined the asperity boundaries as the 3.5 m slip contour of the 2014 earthquake (Duputel et al., 2015; Figure 3a). Results show that after 200 years of loading, positive Coulomb failure stress (CFS) is accumulated along the rim of the asperity with a maximum of ~17 MPa at the downdip margin. This region correlates well with the updip limit of the interseismic earthquake activity. The foreshocks skirt the upper rim that also shows increased CFS (Figure 3a). The region updip of the asperity is shielded and slips at a much lower rate producing a partially kinematically locked zone that extends significantly further updip than the fully coupled asperity (blue contours in Figure 3a; Almeida et al., 2018; Herman et al., 2018). This zone was seismically quiet until the foreshock sequence started.

3. Discussion

We interpret the patch of high coseismic slip, which was locked and seismically quiet in the years prior to the earthquake, as the main asperity responsible for the 2014 Iquique earthquake. Guided by our modeling results, we explain the spatiotemporal distribution of seismicity and modes of slip in the Iquique earthquake region with a simple conceptual model. We note that a similar model was suggested by Dmowska and Li (1982) almost four decades ago, when observational capabilities did not allow verification to the level of detail possible today. Consider a subducting slab that is coupled to the upper plate across an elliptical patch but is allowed to creep elsewhere (Figure 4). As the clamped asperity subducts, strain builds up around the asperity with a maximum along its downdip margin (Figure 4), as a result of the downgoing motion of the asperity and the increase of normal stress with depth. In the strained and stressed regions we expect earthquakes, as the real megathrust is not as homogeneous as our models and movement is likely accompanied by microseismicity and earthquake repeaters. This is what we observe in the years preceding the Iquique event, where earthquakes and repeaters occur on the plate interface in front of the asperity relatively continuously. Strain is also expected along the asperity's flanks (north and south), where earthquakes do occur, although more clustered in space and time (Figures 2a and 2b). Socquet et al. (2017) found accelerated aseismic slip starting 8 months before the mainshock on either side of the asperity (Figure 2a) in accordance with the seismicity clusters. Approximately, the same regions showed also the bulk of postseismic slip (Hoffmann et al., 2018; Shrivastava et al., 2019; Figure 2a), indicating that the subduction fault moves

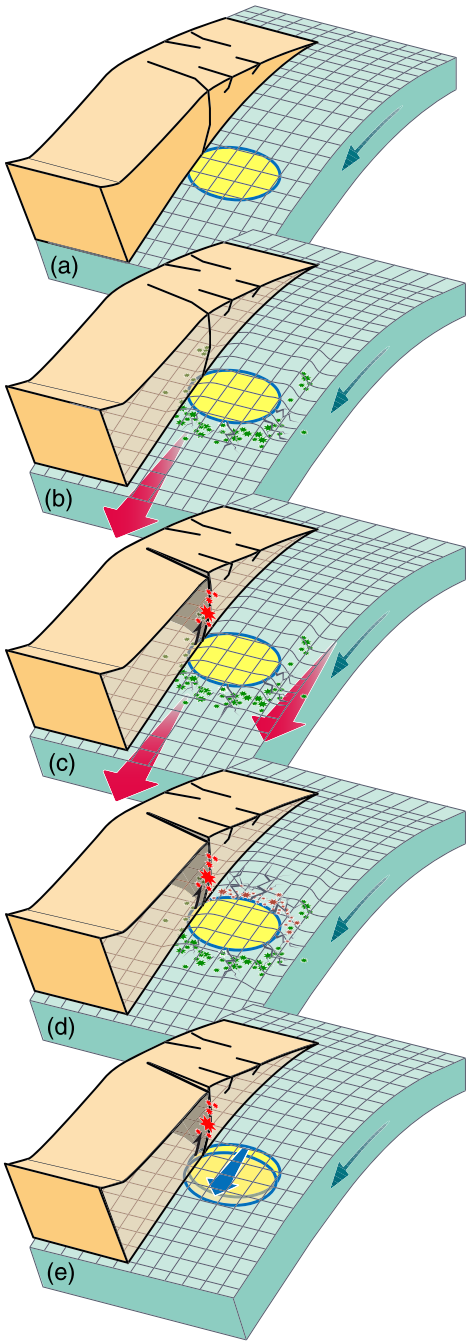

Figure 4. Conceptual model explaining observations of spatiotemporal behavior of preevent seismicity. (a) Upper and lower plate are locked across an elliptical asperity (yellow) and allowed to creep everywhere else. (b) As lower plate subducts, strain downdip and to the sides of the asperity, whereas the region updip of the asperity is shielded. Seismicity occurs in the stressed regions. (c) If plates are locked strongly across asperity, the upper plate may break first in order to relax the system. (d) Seismicity infringes onto the plate interface updip of the asperity and closes the "Mogi-doughnut." (e) Asperity breaks in mainshock.

here at least in part aseismically and that a phase of creep around the asperity may have begun in the months before the mainshock, further stressing the asperity's margins.

What is the significance of the first upper plate foreshock in relation to the following preseismic interplate sequence that closed the "Mogi doughnut" around the updip half of the asperity? This region of the plate interface was seismically quiet for 7 years until 2 weeks before the mainshock. Here the coupled patch is expected to cast a stress shadow (Figure 3) (Almeida et al., 2018; Bürgmann et al., 2005; Herman et al., 2018; Hetland & Simons, 2010; Wang & Tréhu, 2016) generally inhibiting fault movement. Accumulated elastic strain eventually gets relaxed by breaking the weakest part of the system, which generally constitutes the megathrust fault in subduction zones. However, if the asperity is particularly strong, strain may, at least partly, be relaxed by breaking the upper plate. The first large foreshock occurred updip and above the asperity where modeling predicts significantly increased shear tractions on planes comparable to the foreshock mechanism (Figure S11). Forearc wedges are known to contain splay faults, and one of these may have ruptured before the megathrust. Our modeling shows that interseismic CFS on the megathrust was increased along the asperity's upper edge (Figures 3a and S10e). An additional slight increase induced by the upper plate foreshock (González et al., 2015; Herman et al., 2015) might have triggered the preseismic sequence along the prestressed upper rim. Updip, normal stress is also decreased (Figure S10f), lowering friction and possibly promoting stable slip in a conditionally stable environment (Scholz, 1998). Repeating events (Kato et al., 2016; Kato & Nakagawa, 2014; Meng et al., 2015; Figure 2) and observed GPS surface displacement transients (Bedford et al., 2015; Herman et al., 2015; Ruiz et al., 2014) during the foreshock sequence suggest that aseismic slip was accompanying or even driving the preseismic activity. Dynamic seismic cycle simulations using rate-and-state friction laws showed that frictionally locked asperities get eroded at the margins by creep penetrating at the late stage of the seismic cycle (Hori & Miyazaki, 2010; Lapusta & Liu, 2009; Mavrommatis et al., 2017). Our observed interseismic and preseismic activity is likely an expression of this dynamic erosion process around asperities.

The completion of the Mogi Doughnut around the Iquique earthquake might be a special case. Here, stresses in the upper plate that likely resulted from crustal heterogeneity were released and projected by foreshocks onto a portion of the megathrust that would otherwise be in a stress shadow. This triggered further foreshocks now on the megathrust that closed the "doughnut." The downdip half, however, maybe symptomatic for critically stressed asperities. We consider it worthwhile to search for such crescent-shaped patterns of seismicity as illustrated in Figure 1a) along well-monitored seismic gaps to identify asperities in conjunction with geodetic measurements.

What causes the Iquique asperity, and is it ephemeral or does it persist over multiple earthquake cycles? Figure 3b shows the residual gravity field (Figure S12) and several of our observed and modeled attributes. The coseismic slip high is correlated with an ~40 mgal gravity low encircled by a relative gravity high that is correlated with the Mogi doughnut seismicity. The correlation between the residual gravity anomalies and the Iquique earthquake sequence indicates geological control on interplate coupling. A rough subducting plate has been associated with fracturing of the upper plate and a weak plate boundary (see review by Wang & Bilek, 2014), and Geersen

et al. (2015) have interpreted seismic reflection data to indicate subducted seamounts beneath the upper plate wedge, consistent with the observations of a rough plate seaward of the trench. Because of the relatively high density of oceanic crust compared to most forearc wedge materials, seamounts should produce forearc gravity highs. The high gravity ring that corresponds to the "Mogi doughnut" identified in this paper may result, at least in part, from topography on the subducted plate. However, we note that the gravity low also correlates with a recent sedimentary basin (Figures S13 and S14). The presence of this basin must contribute significantly to the gravity anomaly; in a simple two-body gravity calculation an 800-m-thick basin with a density contrast of -500 km/m^3 would produce a gravity low with an amplitude of ~15 mgal. Initiation of the mainshock at the edge of a gravity low and the close correspondence between the patch of greatest slip and the low is consistent with a global pattern first recognized by Wells et al. (2003) and Song and Simons (2003). Wells et al. (2003) interpreted the correlation between slip and gravity lows to indicate basal erosion of the upper plate in response to locally high friction on these patches of the megathrust, an association that is supported by our observations. The fundamental geologic reason for these associations, however, remains enigmatic.

4. Conclusions

Seismicity preceding the 2014 *M*8.1 Iquique earthquake formed a distinct ring around a quiet zone, a pattern known as a Mogi doughnut. The downdip half of the doughnut was activated during the 7-year observation period leading up the event, whereas its updip half was formed during a 2-week-long foreshock sequence initiated by a *M*6.7 upper plate event. The doughnut's hole broke with up to 12 m of slip in the mainshock. There is a striking correlation between the premainshock quiet region, the patch of strongest interseismic locking, the coseismic high-slip patch, and a pronounced forearc gravity low. Together, these observations provide a rare opportunity to locate a major subduction zone asperity with high confidence. The gravity data imply that this asperity is persistent and related to crustal structure, although the details of this structure cannot be constrained by gravity data alone. Mechanical modeling of asperity loading shows that CFS accumulates around the asperity where we observed interseismic and preseismic activity. Most features of the spatiotemporal seismicity pattern can be well explained by stress accumulation on the asperity as subduction is driven by relative plate motion. These observations may provide clues to the future behavior of other well monitored subduction zone segments.

Data Availability Statement

The catalog of relocated seismicity generated and analyzed in this study as well as the interseismic locking and gravity map can be accessed from Schurr et al. (2020). Seismic waveform data were taken from networks CX (GFZ German Research Centre for Geosciences & Institut des Sciences de l'Univers-Centre National de la Recherche CNRS-INSU, 2006), IQ (Cesca et al., 2009), and GE (GEOFON Data Centre, 1993) accessed via EIDA webservices (e.g., https://geofon.gfz-potsdam.de/), as well as from Chilean Seismological Network (C, C1) stations (Barrientos, 2018) accessed via IRIS webservices (http://ds.iris.edu/SeismiQuery/).

Acknowledgments

We thank the IPOC initiative collecting the high-quality seismic and geodetic data. A. M. T. thanks the U.S. National Science Foundation for support through Grants OCE-1130013 and OCE-1459368, the participants of cruise MGL1610 for assistance in acquiring and processing the seismic reflection data, and Alexander de Moor for his assistance in developing the software to process the gravity data. M. M. acknowledges support from Fondo Nacional de Desarrollo Científico y Tecnológico (1181479), ANILLO (ACT192169), Millennium Nucleus (NC160025), and CONICYT/FONDAP (15110017) projects. We are grateful for the constructive revisions of two anonymous reviewers.

References

Aagaard, B., Kientz, S., Knepley, M., Somala, S., Strand, L., & Williams, C. (2016). *Pylith user manual, version 1.9.0. Computational Infrastructure for Geodynamics (CIG).* Davis: University of California. http://www.geodynamics.org/cig/software/pylith/pylith-manual.pdf

Almeida, R., Lindsey, E. O., Bradley, K., Hubbard, J., Mallick, R., & Hill, E. M. (2018). Can the updip limit of frictional locking on megathrusts be detected geodetically? Quantifying the effect of stress shadows on near-trench coupling. *Geophysical Research Letters*, *45*, 4754–4763. https://doi.org/10.1029/2018GL077785

Barrientos, S. (2018). The seismic network of Chile. *Seismological Research Letters*, *89*(2A), 467–474. https://doi.org/10.1785/0220160195

Bedford, J., Moreno, M., Schurr, B., Bartsch, M., & Oncken, O. (2015). Investigating the final seismic swarm before the Iquique-Pisagua 2014 *Mw*8.1 by comparison of continuous GPS and seismic foreshock data. *Geophysical Research Letters*, *42*, 3820–3828. https://doi.org/10.1002/2015GL063953

Béjar-Pizarro, M., Socquet, A., Armijo, R., Carrizo, D., Genrich, J., & Simons, M. (2013). Andean structural control on interseismic coupling in the North Chile subduction zone. *Nature Geoscience*, *6*(6), 462–467. https://doi.org/10.1038/ngeo1802

Bürgmann, R., Kogan, M. G., Steblov, G. M., Hilley, G., Levin, V. E., & Apel, E. (2005). Interseismic coupling and asperity distribution along the Kamchatka subduction zone. *Journal of Geophysical Research*, *110*, B07405. https://doi.org/10.1029/2005JB003648

Cesca, S., Sobiesiak, M., Tassara, A., Olcay, M., Günther, E., Mikulla, S., & Dahm, T. (2009). The Iquique local network and PicArray. GFZ Data Services. https://doi.org/10.14470/VD070092

Chlieh, M., Perfettini, H., Tavera, H., Avouac, J. P., Remy, D., Nocquet, J. M., et al. (2011). Interseismic coupling and seismic potential along the Central Andes subduction zone. *Journal of Geophysical Research*, *116*, B12405. https://doi.org/10.1029/2010JB008166

GEOFON Data Centre (1993). GEOFON seismic network. Deutsches GeoForschungsZentrum GFZ. Other/Seismic Network. https://doi.org/10.14470/TR560404

Dmowska, R., & Li, V. C. (1982). A mechanical model of precursory source processes for some large earthquakes. *Geophysical Research Letters*, *9*(4), 393–396. https://doi.org/10.1029/GL009i004p00393

Dmowska, R., & Lovison, L. C. (1992). Influence of asperities along subduction interfaces on the stressing and seismicity of adjacent areas. *Tectonophysics*, *211*(1–4), 23–43. https://doi.org/10.1016/0040-1951(92)90049-C

Duputel, Z., Jiang, J., Jolivet, R., Simons, M., Rivera, L., Ampuero, J. P., et al. (2015). The Iquique earthquake sequence of April 2014: Bayesian modeling accounting for prediction uncertainty. *Geophysical Research Letters*, *42*, 7949–7957. https://doi.org/10.1002/2015GL065402

Geersen, J., Ranero, C. R., Barckhausen, U., & Reichert, C. (2015). Subducting seamounts control interplate coupling and seismic rupture in the 2014 Iquique earthquake area. *Nature Communications*, *6*(1), 8267–8267. https://doi.org/10.1038/ncomms9267

GFZ German Research Centre For Geosciences, Institut Des Sciences De L'Univers-Centre National De La Recherche CNRS-INSU (2006). IPOC seismic network, https://doi.org/10.14470/pk615318

González, G., Salazar, P., Loveless, J. P., Allmendinger, R. W., Aron, F., & Shrivastava, M. N. (2015). Upper plate reverse fault reactivation and the unclamping of the megathrust during the 2014 northern Chile earthquake sequence. *Geology*, *43*(8), 671–674. https://doi.org/10.1130/G36703.1

Hayes, G. P., Herman, M. W., Barnhart, W. D., Furlong, K. P., Riquelme, S., Benz, H. M., et al. (2014). Continuing megathrust earthquake potential in Chile after the 2014 Iquique earthquake. *Nature*, *512*(7514), 295–298. https://doi.org/10.1038/nature13677

Hayes, G. P., Wald, D. J., & Johnson, R. L. (2012). Slab1.0: A three-dimensional model of global subduction zone geometries. *Journal of Geophysical Research*, *117*, B01302. https://doi.org/10.1029/2011JB008524

Herman, M. W., Furlong, K. P., & Govers, R. (2018). The accumulation of slip deficit in Subduction zones in the absence of mechanical coupling: Implications for the behavior of megathrust earthquakes. *Journal of Geophysical Research: Solid Earth*, *123*, 8260–8278. https://doi.org/10.1029/2018JB016336

Herman, M. W., Furlong, K. P., Hayes, G. P., & Benz, H. M. (2015). Foreshock triggering of the 1 April 2014 *Mw* 8.2 Iquique, Chile, earthquake. *Earth and Planetary Science Letters*, *447*(April 2014), 119–129. https://doi.org/10.1016/j.epsl.2016.04.020

Hetland, E. A., & Simons, M. (2010). Post-seismic and interseismic fault creep II: Transient creep and interseismic stress shadows on megathrusts. *Geophysical Journal International*, *181*(1), 99–112. https://doi.org/10.1111/j.1365-246X.2009.04482.x

Hoffmann, F., Metzger, S., Moreno, M., Deng, Z., Sippl, C., Ortega-Culaciati, F., & Oncken, O. (2018). Characterizing afterslip and ground displacement rate increase following the 2014 Iquique-Pisagua *Mw*8.1 earthquake, northern Chile. *Journal of Geophysical Research: Solid Earth*, *123*, 4171–4192. https://doi.org/10.1002/2017JB014970

Hori, T., & Miyazaki, S. (2010). Hierarchical asperity model for multiscale characteristic earthquakes: A numerical study for the off-Kamaishi earthquake sequence in the NE Japan subduction zone. *Geophysical Research Letters*, *37*, L10304. https://doi.org/10.1029/2010GL042669

Husen, S., Kissling, E., Flueh, E. R., & Asch, G. (1999). Accurate hypocentre determination in the seismogenic zone of the subducting Nazca Plate in northern Chile using a combined on-/offshore network. *Geophysical Journal International*, *138*(3), 687–701. https://doi.org/10.1046/j.1365-246x.1999.00893.x

Igarashi, T., Matsuzawa, T., & Hasegawa, A. (2003). Repeating earthquakes and interplate aseismic slip in the northeastern Japan subduction zone. *Journal of Geophysical Research*, *108*(B5), 2249. https://doi.org/10.1029/2002JB001920

Jara, J., Sánchez-Reyes, H., Socquet, A., Cotton, F., Virieux, J., Maksymowicz, A., et al. (2018). Kinematic study of Iquique 2014 *Mw* 8.1 earthquake: Understanding the segmentation of the seismogenic zone. *Earth and Planetary Science Letters*, *503*, 131–143. https://doi.org/10.1016/j.epsl.2018.09.025

Jolivet, R., Simons, M., Duputel, Z., Olive, J. A., Bhat, H. S., & Bletery, Q. (2020). Interseismic loading of subduction megathrust drives long-term uplift in northern Chile. *Geophysical Research Letters*, *47*, e2019GL085377. https://doi.org/10.1029/2019GL085377

Kanamori, H. (1981). The nature of seismicity patterns before large earthquakes. In D. W. Simpson & P. G. Richards (Eds.), *Earthquake prediction: An international review*, *Maurice Ewing Series* (Vol. 4, pp. 1–19). Washington DC: American Geophysical Union. https://doi.org/10.1029/ME004p0001

Kanda, R. V. S., & Simons, M. (2010). An elastic plate model for interseismic deformation in subduction zones. *Journal of Geophysical Research*, *115*, B03405. https://doi.org/10.1029/2009JB006611

Kato, A., Fukuda, J., Kumazawa, T., & Nakagawa, S. (2016). Accelerated nucleation of the 2014 Iquique, Chile *Mw* 8.2 earthquake. *Scientific Reports*, *6*(1), 1–9. https://doi.org/10.1038/srep24792

Kato, A., & Nakagawa, S. (2014). Multiple slow-slip events during a foreshock sequence of the 2014 Iquique, Chile *Mw* 8.1 earthquake. *Geophysical Research Letters*, *41*, 5420–5427. https://doi.org/10.1002/2014GL061138

Kendrick, E., Bevis, M., Smalley, R., & Brooks, B. (2001). An integrated crustal velocity field for the central Andes. *Geochemistry, Geophysics, Geosystems*, *2*(11), 1066. https://doi.org/10.1029/2001GC000191

Lapusta, N., & Liu, Y. (2009). Three-dimensional boundary integral modeling of spontaneous earthquake sequences and aseismic slip. *Journal of Geophysical Research*, *114*, B09303. https://doi.org/10.1029/2008JB005934

Lay, T., & Kanamori, H. (1981). An asperity model of large earthquake sequences. In D. W. Simpson & P. G. Richards (Eds.), *Earthquake prediction: An international review*, *Maurice Ewing Series* (Vol. 4, pp. 579–592). Washington DC: American Geophysical Union.

Lay, T., Yue, H., Brodsky, E. E., & An, C. (2014). The 1 April 2014 Iquique, Chile, *Mw* 8.1 earthquake rupture sequence. *Geophysical Research Letters*, *41*, 3818–3825. https://doi.org/10.1002/2014GL060238

Li, S., Moreno, M., Bedford, J., Rosenau, M., & Oncken, O. (2015). Revisiting viscoelastic effects on interseismic deformation and locking degree: A case study of the Peru-North Chile subduction zone. *Journal of Geophysical Research: Solid Earth*, *120*, 4522–4538. https://doi.org/10.1002/2015JB011903

Li, S., Wang, K., Wang, Y., Jiang, Y., & Dosso, S. E. (2018). Geodetically inferred locking state of the Cascadia megathrust based on a viscoelastic Earth model. *Journal of Geophysical Research: Solid Earth*, *123*, 8056–8072. https://doi.org/10.1029/2018JB015620

Mavrommatis, A. P., Segall, P., & Johnson, K. M. (2017). A physical model for interseismic erosion of locked fault asperities. *Journal of Geophysical Research: Solid Earth*, *122*, 8326–8346. https://doi.org/10.1002/2017JB014533

Meng, L., Huang, H., Bürgmann, R., Ampuero, J. P., & Strader, A. (2015). Dual megathrust slip behaviors of the 2014 Iquique earthquake sequence. *Earth and Planetary Science Letters*, *411*, 177–187. https://doi.org/10.1016/j.epsl.2014.11.041

Métois, M., Socquet, A., Vigny, C., Carrizo, D., Peyrat, S., Delorme, A., et al. (2013). Revisiting the North Chile seismic gap segmentation using GPS-derived interseismic coupling. *Geophysical Journal International*, *194*(3), 1283–1294. https://doi.org/10.1093/gji/ggt183

Métois, M., Vigny, C., & Socquet, A. (2016). Interseismic coupling, megathrust earthquakes and seismic swarms along the Chilean subduction zone (38°–18°S). *Pure and Applied Geophysics*, *173*(5), 1431–1449. https://doi.org/10.1007/s00024-016-1280-5

Mogi, K. (1969). Some features of recent seismic activity in and near Japan (2) activity before and after great earthquakes. *Bulletin of the Earthquake Research Institute*, *47*(4), 395–417.

Moreno, M., Li, S., Melnick, D., Bedford, J. R., Baez, J. C., Motagh, M., et al. (2018). Chilean megathrust earthquake recurrence linked to frictional contrast at depth. *Nature Geoscience*, *11*(4), 285–290. https://doi.org/10.1038/s41561-018-0089-5

Nábělek, J. L., & Xia, G. (1995). Moment-tensor analysis using regional data: Application to the 25 March, 1993, Scotts Mills, Oregon, earthquake. *Geophysical Research Letters*, *22*(1), 13–16. https://doi.org/10.1029/94GL02760

Ruiz, J., Maksymowicz, A., Ortega-Culaciati, F., Rivera, L., & Comte, D. (2019). Source characteristics of the March 16, 2014 *Mw* 6.7 earthquake and its implications for the *Mw* 8.2 Pisagua mainshock. *Tectonophysics*, *767*, 228170. https://doi.org/10.1016/j.tecto.2019.228170

Ruiz, S., & Madariaga, R. (2018). Historical and recent large megathrust earthquakes in Chile. *Tectonophysics*, *733*, 37–56. https://doi.org/10.1016/j.tecto.2018.01.015

Ruiz, S., Metois, M., Fuenzalida, A., Ruiz, J., Leyton, F., Grandin, R., et al. (2014). Intense foreshocks and a slow slip event preceded the 2014 Iquique *Mw*8.1 earthquake. *Science*, *345*(6201), 1165–1169. https://doi.org/10.1126/science.1256074

Savage, J. C. (1983). A dislocation model of strain accumulation and release at a subduction zone. *Journal of Geophysical Research*, *88*(B6), 4984–4996. https://doi.org/10.1029/JB088iB06p04984

Scholz, C. H. (1998). Earthquakes and friction laws. *Nature*, *391*(6662), 37–42. https://doi.org/10.1038/34097

Schurr, B., Asch, G., Hainzl, S., Bedford, J., Hoechner, A., Palo, M., et al. (2014). Gradual unlocking of plate boundary controlled initiation of the 2014 Iquique earthquake. *Nature*, *512*(7514), 299–302. https://doi.org/10.1038/nature13681

Schurr, B., Asch, G., Rosenau, M., Wang, R., Oncken, O., Barrientos, S. E., et al. (2012). The 2007 *M*7.7 Tocopilla northern Chile earthquake sequence: Implications for along-strike and downdip rupture segmentation and megathrust frictional behavior. *Journal of Geophysical Research*, *117*, B05305. https://doi.org/10.1029/2011JB009030

Schurr, B., Moreno, M., Tréhu, A. M., Bedford, J., Kummerow, J., Li, S., & Oncken, O. (2020). Pre-seismic earthquake catalog, inter-seismic locking model, and corrected gravity field for the 2014 M8.1 Iquique, northern Chile, earthquake rupture region. GFZ Data Services. https://doi.org/10.5880/GFZ.4.1.2020.011

Shrivastava, M. N., González, G., Moreno, M., Soto, H., Schurr, B., Salazar, P., & Báez, J. C. (2019). Earthquake segmentation in northern Chile correlates with curved plate geometry. *Scientific Reports*, *9*(1), 4403. https://doi.org/10.1038/s41598-019-40282-6

Sippl, C., Schurr, B., Asch, G., & Kummerow, J. (2018). Seismicity structure of the northern Chile forearc from >100,000 double-difference relocated hypocenters. *Journal of Geophysical Research: Solid Earth*, *123*, 4063–4087. https://doi.org/10.1002/2017JB015384

Sippl, C., Schurr, B., Yuan, X., Mechie, J., Schneider, F. M., Gadoev, M., et al. (2013). Geometry of the Pamir-Hindu Kush intermediate-depth earthquake zone from local seismic data. *Journal of Geophysical Research: Solid Earth*, *118*, 1438–1457. https://doi.org/10.1002/jgrb.50128

Socquet, A., Valdes, J. P., Jara, J., Cotton, F., Walpersdorf, A., Cotte, N., et al. (2017). An 8 month slow slip event triggers progressive nucleation of the 2014 Chile megathrust. *Geophysical Research Letters*, *44*, 4046–4053. https://doi.org/10.1002/2017GL073023

Song, T. R. A., & Simons, M. (2003). Large trench-parallel gravity variations predict seismogenic behavior in subduction zones. *Science*, *301*(5633), 630–633. https://doi.org/10.1126/science.1085557

Soto, H., Sippl, C., Schurr, B., Kummerow, J., Asch, G., Tilmann, F., et al. (2019). Probing the northern Chile megathrust with seismicity: The 2014 *M*8.1 Iquique earthquake sequence. *Journal of Geophysical Research: Solid Earth*, *124*, 12,935–12,954. https://doi.org/10.1029/2019JB017794

Tassara, A., & Echaurren, A. (2012). Anatomy of the Andean subduction zone: Three-dimensional density model upgraded and compared against global-scale models. *Geophysical Journal International*, *189*(1), 161–168. https://doi.org/10.1111/j.1365-246X.2012.05397.x

Thatcher, W. (1990). Order and diversity in the modes of Circum-Pacific earthquake recurrence. *Journal of Geophysical Research*, *95*(B3), 2609. https://doi.org/10.1029/JB095iB03p02609

Tilmann, F. J., Zhang, Y., Moreno, M., Saul, J., Eckelmann, F., Palo, M., et al. (2016). The 2015 Illapel earthquake, central Chile: A type case for a characteristic earthquake? *Geophysical Research Letters*, *43*, 574–583. https://doi.org/10.1002/2015GL066963

Waldhauser, F., & Ellsworth, W. L. (2000). A double-difference earthquake location algorithm: Method and application to the northern Hayward Fault, California. *Bulletin of the Seismological Society of America*, *90*(6), 1353–1368. https://doi.org/10.1785/0120000006

Wang, K., & Bilek, S. L. (2014). Invited review paper: Fault creep caused by subduction of rough seafloor relief. *Tectonophysics*, *610*, 1–24. https://doi.org/10.1016/j.tecto.2013.11.024

Wang, K., & Tréhu, A. M. (2016). Some outstanding issues in the study of great megathrust earthquakes—The Cascadia example. *Journal of Geodynamics*, *98*, 1–18. https://doi.org/10.1016/j.jog.2016.03.010

Wells, R. E., Blakely, R. J., Sugiyama, Y., Scholl, D. W., & Dinterman, P. A. (2003). Basin-centered asperities in great subduction zone earthquakes: A link between slip, subsidence, and subduction erosion? *Journal of Geophysical Research*, *108*(B10), 2507. https://doi.org/10.1029/2002JB002072

Yagi, Y., Okuwaki, R., Enescu, B., Hirano, S., Yamagami, Y., Endo, S., & Komoro, T. (2014). Rupture process of the 2014 Iquique Chile earthquake in relation with the foreshock activity. *Geophysical Research Letters*, *41*, 4201–4206. https://doi.org/10.1002/2014GL060274

Yamanaka, Y., & Kikuchi, M. (2004). Asperity map along the subduction zone in northeastern Japan inferred from regional seismic data. *Journal of Geophysical Research*, *109*, B07307. https://doi.org/10.1029/2003JB002683

References From the Supporting Information

Aagaard, B. T., Knepley, M. G., & Williams, C. A. (2013). A domain decomposition approach to implementing fault slip in finite-element models of quasi-static and dynamic crustal deformation. *Journal of Geophysical Research: Solid Earth*, *118*, 3059–3079. https://doi.org/10.1002/jgrb.50217

Blakely, R. J. (1996). *Potential theory in gravity and magnetic applications*. Cambridge, UK: Cambridge University Press.

Contreras-Reyes, E., Jara, J., Grevemeyer, I., Ruiz, S., & Carrizo, D. (2012). Abrupt change in the dip of the subducting plate beneath north Chile. *Nature Geoscience*, *5*(5), 342–345. https://doi.org/10.1038/ngeo1447

De Moor, A. (2015). *Local seismicity recorded by ChilePEPPER: Implications for dynamic accretionary prism response and long-term prism evolution* (MS thesis, p. 79). Oregon State University. Retrieved from https://ir.library.oregonstate.edu/xmlui/handle/1957/58092

González, E. (1989). Hydrocarbon resources in the coastal zone of Chile. In G. E. Ericksen, M. T. Canas Pinochet, & J. A. Reinemund(Eds.), *Geology of the Andes and its relation to hydrocarbon and mineral resources* (pp. 383–404). Houston, TX: Circum Pacific Council Publications.

Moberly, R., Shepherd, G. L., & Coulbourn, W. T. (1982). Forearc and other basins, continental margin of northern and southern Peru and adjacent Ecuador and Chile. *Geological Society, London, Special Publications*, *10*, 171–189. https://doi.org/10.1144/GSL.SP1982.010.01.11

Tréhu, A.M., Vera, E., Riedel, M., & MGL1610 Science Party. (2017). MGL1610 Cruise Report, https://www.rvdata.us/search/cruise/MGL1610